International Journal of Research in Engineering and Science (IJRES)
ISSN (Online): 2320-9364, ISSN (Print): 2320-9356
www.ijres.org Volume 9 Issue 7 ǁ 2021 ǁ PP. 26-32

Segmentation of Head and Neck Cancer cell using Deep learning

[1]Ramadhuvishan A., [2]Mohammed Mufassal Sultan P M
[3]Pon Aravind B, [4]Kamalesh S, [5]Perumalraja R

*[*1]Department of Information Technology, Velammal College of Engineering and Technology, Madurai - 09*
[2] Department of Information Technology, Velammal College of Engineering and Technology, Madurai - 09
[3] Department of Information Technology, Velammal College of Engineering and Technology, Madurai – 09
[4] Department of Information Technology, Velammal College of Engineering and Technology, Madurai – 09
[5] Department of Information Technology, Velammal College of Engineering and Technology, Madurai – 09

Abstract
Every year the number of Head and Neck Cancer (HNC) increases rapidly. Segmentation of the Cancer cells of Head and Neck parts is always a time consuming process that needs a minimum of 4 hours time for a single patient by an 'expertized oncologist'. Deep learning has always been an important tool for medical image processing, thus implementing a Deep learning based algorithm for the segmentation of Cancer cells from the normal cells will be a great help in the Oncological department. We've proposed an Enhanced 3D Generative Adversarial Network (GAN). As GAN is an Unsupervised learning algorithm thus will be a very great tool in the process of segmentation, and as the working of GAN is an iterative learning process thus the results produced form GAN based models are a good supporting tool. From the dataset we acquired from AI Crowd HECKTOR Challenge, we've produced a dice score of 0.8085.

Keywords: *Auto segmentation, HNC, Enhanced 3D GAN, Radiotherapy, Oncology*

Date of Submission: 13-07-2021 Date of acceptance: 29-07-2021

I. Introduction

Every year, over a half a million people are diagnosed with head and cancer worldwide. This incidence is rising , more than doubling in certain subgroups over the last 30 years[3].Where available,most will be treated with radiotherapy which targets the tumour mass. However, good strategies are needed so that only the affected cells (tumor) are
irradiated , if mishandled they may irradiate organs that are normal anatomical structures.

The efficacy and safety of head and neck radiotherapy thus depends upon the accurate delineation of tumour, a process known as segmentation or contouring. The expertised oncologist are only involved in such a process, as this segmentation process is done manually, which may result in both inconsistent and imperfectly accurate [10,11].

Fig. 1: A typical clinical pathway for radiotherapy.

An expert spends four hours or more on a single case for the segmentation process alone (see Fig. 1) [12]. This delay becomes a great hazard when it comes to the number of cases and/ or the deadliness of the case [13]. Also the demand for an expertised oncologist and radiographers has been increasing for the past few decades, along with the previous delay and the demand for the expertized may result in long delays for patients [4, 15, 16]. This process lies as a hurdle in the case of "Adaptive radiotherapy" (Process of repeated scanning, segmentation and radiotherapy planning).

II. Literature survey

Previous works of HNC segmentation using deep learning works have been carried from more than the last decade. The previous works of deep learning based algorithms that have been carried out using a standard

CNN have proven capable of delivering substantially better performance than the traditional segmentation algorithms. However the Unet Convolutional architecture has shown promise in the area of deep learning based medical image segmentation.

As the processing of Tomography images using the deep learning approaches in the past years, experts converted the 3D formats of tomography images to easily readable 2D formats thus produced a model for the segmentation and with that they've acquired an accuracy of 0.9987 using a 2D Unet model. Even Though the accuracy of the segmentation process using the 2D Unet model is comparatively high, the slicing of the tomography may cause some losses in the spatial dimension.

An automatic segmentation algorithm for delineation of the gross tumour volume and pathologic lymph nodes of head and neck cancers in PET/CT images is described. The proposed algorithm is based on a convolutional neural network using the U-Net architecture. [18,20]

A U Net based deep learning algorithm , that uses 3D convolutions instead of normal convolutions called 3D UNet , which segments organs at risk (OARs). The delineates 21 OARs given a CT scan of a patient[19]. The model showed near accuracy of expert radiographer's with non-substantial difference of +5 to -5% [19].

The Pix2Pix GAN is a general approach for image-to-image translation. It is based on the conditional generative adversarial network, where a target image is generated, conditional on a given input image. The Pix2Pix GAN changes the loss function so that the generated image is both plausible in the content of the target domain, and is a plausible translation of the input image [24].

Thus, To understand segmentation, conversion of images GAN is used as the state of the art tool, so applying the same for the medical images we can achieve at a finer results as compared to the previous works.

Segmentation using 3D pix2pix ,i.e., vox2vox has been applied and the model attained dice scores of 90.66%, 82.54%, 78.71% for the BraTS 2018 same vox2vox applied for our dataset.[22]

III. Methods and Methodologies

3.1. Data preprocessing

The training data comprises 201 cases from four centers (CHGJ, CHMR, CHUM and CHUS). The test data comprise 53 cases from another center (CHUV).Each case comprises: CT, PET and GTVt (primary Gross Tumor Volume) in NIfTI format, as well as the bounding box location and patient information [1,2,3].

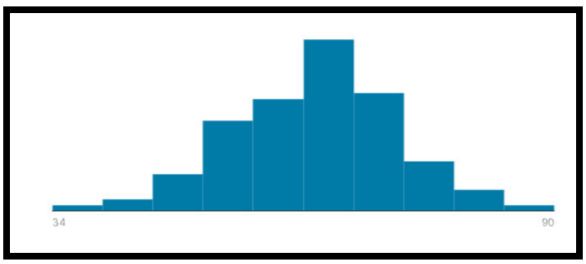

Fig. 2: Age distribution of the patients

We use the official bounding box to crop all the images. We also resample the images to isotropic resolution 1mmx1mmx1mm. All the scans are resampled to the shape 144x144x144. After resampling, for better generalization of the model the data is augmented by various methods [23].

We normalized the data using Minimum and Maximum Hounsfield values.

p.i. < H_MIN:
p.i. = H_MIN
p.i. > H_MAX:
p.i. = H_MAX
$p.i._{(N)} = (p.i.-H\_MIN) / (H\_MAX-H\_MIN)$
Where,
p.i. - Pixel Intensity
H_MIN - Hounsfield Minimum
H_MAX - Hounsfield Maximum
$p.i._{(N)}$ - Normalized Pixel Intensity

3.2. GAN

A GAN is a class of Machine Learning frameworks that is proposed for an unsupervised learning. The main ideology behind the GAN is two Neural networks namely, Generator and Discriminator contest with each other to win over the other.

3.3. 3D GAN Architecture

Fig. 2: Simple Block Diagram of CNN

A CNN model is trained on various layers of networks so that the model acquired from a CNN is an expert in the segmentation field. But due to it's flow of working there isn't any feedback procedure for the model to learn and arrive at a well expertized system.

Whereas the 3D GAN model is a two networks namely Generator and Discriminator, trying to dominate each other, i.e., the Generator keeps on producing the images and those will be evaluated by the Discriminator to say whether those produced images are fake or real. Once the discriminator gets failed, the model is said to be an expertized model. Thus, in segmentation of medical images the required model will be trained on a 'feedback system' so that the precision of end results will be acceptable.

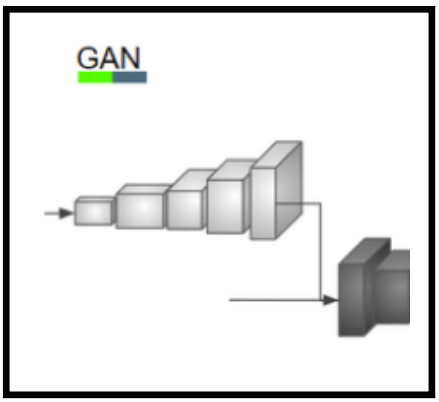

Fig. 3 Simple Block Diagram of GAN

IV. Algorithmic overview [21]

4.1. Pseudo Code

"for number of training iterations **do**

for k steps **do**

- Sample minibatch of m noise samples $\{z^{(1)}, \ldots, z^{(m)}\}$ from noise prior $p_q(z)$.
- Sample minibatch of m noise samples $\{x^{(1)}, \ldots, x^{(m)}\}$ from data generating distribution $p_{data}(x)$.
- Update the discriminator by ascending its stochastic gradient

$$\nabla_{\theta_d} \frac{1}{m} \sum_{i=1}^{m} \left[\log D\left(\boldsymbol{x}^{(i)}\right) + \log\left(1 - D\left(G\left(\boldsymbol{z}^{(i)}\right)\right)\right) \right].$$

end for

- Sample minibatch of m noise samples $\{z^{(1)}, \ldots, z^{(m)}\}$ from noise prior $p_q(z)$.

- Update the generator by descending its stochastic gradient

$$\nabla_{\theta_g} \frac{1}{m} \sum_{i=1}^{m} \log \left(1 - D\left(G\left(\boldsymbol{z}^{(i)}\right)\right)\right).$$

end for

The gradient based updates can use any standard gradient based learning rule. We used momentum in our experiments."[21]

The above pseudocode is an excerpt from the original GAN paper published , which shows the algorithm for a GAN. The GAN training algorithm involves training both the discriminator and the generator model in parallel.

The outer loop of the algorithm involves iterating over steps to train the models in the architecture. One cycle through this loop is not an epoch: it is a single update composed of specific batch updates to the discriminator and generator models.

V. Model Architecture

The Vox2Vox model, as the Pix2Pix one , consists of a generator and a discriminator. **The generator architecture**, illustrated by Figure (see Fig. 4) , is built as U-Net :

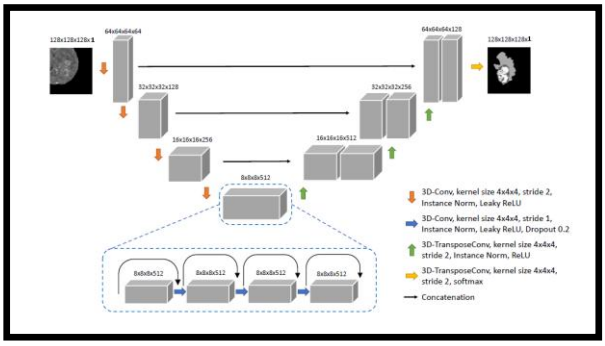

Fig. 4: 3D GAN's Generator Model Architecture

***I*:** a 3D image with 1 channel: ct and gtvt;
***A*:** four 3D convolutions using kernel size 4x4x4, stride 2 and same padding,followed by instance normalization [30] and Leaky ReLU activation function.The number of filters used at the first 3D convolution is 64 and at each down-sampling the number is doubled;
B: four 3D convolutions using kernel size 4x4x4, stride 1 and same padding, followed by instance normalization and Leaky Relu activation function .Every convolution-normalization-activation output is concatenated with the previous one;
C: three 3D transpose convolutions using kernel size 4x4x4 and stride 2, followed by instance normalization and ReLU activation. Each 3D convolution input is concatenated with the respective encoder output layer;
D: segmentation prediction of size 128x128x128x1 given by a 3D transpose convolution using 1 filters , kernel size 4x4x4 and stride 2, followed by softmax activation function generates 1 channel segmentation prediction of the input image.

Discriminator architecture:
I: the 3D image with 1 channel and its segmentation ground-truth or the generator's segmentation prediction;
E: the same of the generator;
D: volume of size 8x8x8x1 given by a 3D convolution using 1 filter, kernel size 4x4x4, stride 1 and same padding generates the discriminator output,used to determine the quality of the segmentation prediction created by the generator.

VI. Hardware and Software requirements

The Hardware requirements for the model is a 16GB RAM processing with a 16GB GPU nVIDIA T4 with a minimum free memory space of 10 GB least.

And for the execution of the model we require a Python 3.6.x - Python 3.7.x versions as they're considered as the stable versions that support most of the libraries. We also require Tensorflow which has the necessary libraries for the creation of the model.

Due to our hardware constraint we've used Google Colaboratory for our work.

VII. Experimental results

We trained our model on 100 datasets and 20 Validation sets and tested with 30 patients from the given test set for the CNN and the 3D GAN models. And we have compared our performance with previous works.

The Qualitative and Comparison of the works have been done in the **Fig. 5 and Fig. 6** and in **Table 1 and 2**.

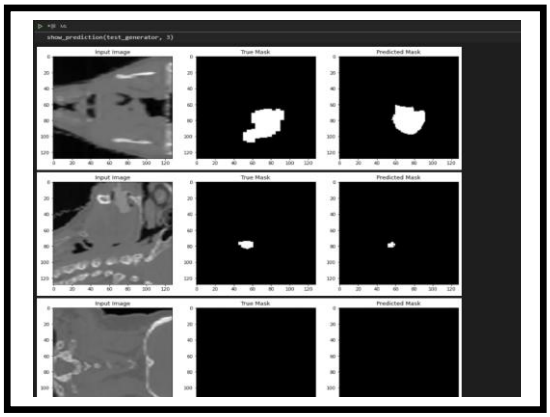

Fig. 5: Qualitative results of Cancer cell detection in 3 different patients using 3D GAN. From left to right, 1st image(s) are the input CT Image, 2nd image(s) are the Given mask for the Cancer cell and the 3rd image(s) are the Predicted mask.

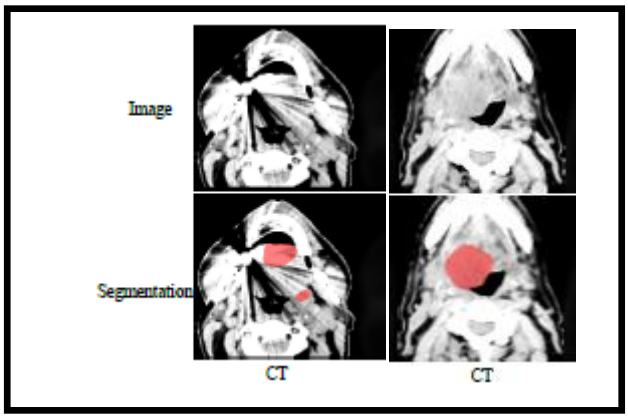

Fig. 6: Qualitative results of UNet based model, the images in the first row are the input CT images and the next two rows are the Segmented Cancer cells.

Table 1: Sample performance table of UNet for the available dataset

Patient ID	DSC	Accuracy	Precision
CHUV001	0.759	0.972	0.838
CHUV002	0.752	0.978	0.834
CHUV003	0.735	0.969	0.833
CHUV004	0.732	0.975	0.833
CHUV005	0.724	0.974	0.829

Table 2: Sample performance table of 3D GAN for the available dataset

Patient ID	DSC	Accuracy	Precision
CHUV001	0.851	0.982	0.801
CHUV002	0.854	0.968	0.811
CHUV003	0.837	0.981	0.821
CHUV004	0.839	0.975	0.820
CHUV005	0.844	0.998	0.810

For achieving generalisability we've also trained our model using the BraTs 2020 dataset [25, 26, 27]. The results have been discussed in the following table (**Table 3**).

Table 3: Mean dice score for the different brain tumour areas over the training set. The metrics here are obtained training the model with sub-volumes of 128 × 128 × 128 voxels, for different values of α = 0, 1, 3, 5, 10. The classes are reset as: whole tumour (WT = ET ∪ ED ∪ NCR/NET), tumour core (TC = ET ∪ NCR/NET) and enhancing tumour (ET)

	DSC		
α	**WT**	**TC**	**ET**
0	0.5986	0.2257	0.3663
1	0.8555	0.7224	0.6250
3	0.9289	0.9088	0.7777
5	0.9421	0.9234	0.8031
10	0.8777	0.8006	0.7155

VIII. Conclusion

Using 3D GAN we have tried to reduce the time taken for the prediction of Cancer cell(s) in the Head and Neck parts of the human body. As a future enhancement the model will be enhanced by doing K-Fold validations to achieve higher accuracy.

References

[1]. Vincent Andrearczyk, Valentin Oreiller, Mario Jreige, Martin Vallières, Joel Castelli, Hesham Elhalawani, Sarah Boughdad, John O. Prior, Adrien Depeursinge. "Overview of the HECKTOR challenge at MICCAI 2020: Automatic Head and Neck Tumor Segmentation in PET/CT". 2021 https://www.aicrowd.com/challenges/miccai-2020-hecktor

[2]. Vincent Andrearczyk, Valentin Oreiller, Martin Vallières, Joel Castelli, Hesham Elhalawani, Mario Jreige, Sarah Boughdad, John O. Prior, Adrien Depeursinge. "Automatic Segmentation of Head and Neck Tumors and Nodal Metastases in PET-CT scans. In: Medical Imaging with Deep Learning." MIDL 2020. https://www.aicrowd.com/challenges/miccai-2020-hecktor

[3]. Cancer Research UK, "Head and neck cancers incidence statistics," Feb. 2018, accessed: 2018-2-8. https://www.aicrowd.com/challenges/miccai-2020-hecktor

[4]. Oxford Cancer Intelligence Unit, "Profile of head and neck cancers in england: Incidence, mortality and survival," National Cancer Intelligence Network, Tech. Rep., 2010.

[5]. A. Jemal, F. Bray, Et. Al., "Global cancer statistics," CA Cancer Journal Clin., vol. 61, no. 2, pp. 69–90, 2011.

[6]. Cancer Research UK, "Head and neck cancers incidence statistics," Feb. 2018, accessed: 2018-2-8.

[7]. National Cancer Intelligence Network, "NCIN data briefing: Potentially HPV-related head and neck cancers," 2012.

[8]. J. J. Caudell, P. E. Schaner, Et. Al., "Dosimetric factors associated with long-term dysphagia after definitive radiotherapy for squamous cell carcinoma of the head and neck," International Journal Radiotherapy Oncology Biology Physics, vol. 76, no. 2, pp. 403–409, 2010.

[9]. C. M. Nutting, J. P. Morden, Et. Al., "Parotid-sparing intensity modulated versus conventional radiotherapy in head and neck cancer (PARSPORT): a phase 3 multicentre randomised controlled trial," Lancet Oncology, vol. 12, no. 2, p.127–136, 2011.

[10]. B. E. Nelms, Et. Al., "Variations in the contouring of organs at risk: test case from a patient with oropharyngeal cancer," International Journal Radiotherapy Oncology Biological Physics, vol. 82, no. 1, pp. 368–378, 2012.

[11]. P. W. J. Voet, M. L. P. Dirkx, Et. Al., "Does atlas-based auto segmentation of neck levels require subsequent manual contour editing to avoid risk of severe target underdosage? a dosimetric analysis," Radiotherapy Oncology, vol. 98, no. 3, pp. 373–377, 2011.

[12]. P. M. Harari, S. Song, and W. A. Tomé, "Emphasizing conformal avoidance versus target definition for IMRT planning in head-and-neck cancer," International Journal of Radiotherapy Oncology Biology Physics, vol. 77, no. 3, pp. 950–958, Jul. 2010.

[13]. Z. Chen, W. King, Et. Al., "The relationship between waiting time for radiotherapy and clinical outcomes: a systematic review of the literature," Radiotherapy Oncology, vol. 87, no. 1, pp. 3–16, 2008.

[14]. J. S. Mikeljevic, R. Haward, Et. Al., "Trends in postoperative radiotherapy delay and the effect on survival in breast cancer patients treated with conservation surgery," British Journal of Cancer, vol. 90, no. 7, pp. 1343–1348, 2004.

[15]. C. E. Round, M. V. Williams, Et. Al., "Radiotherapy demand and activity in england 2006-2020," Clinical Oncology, vol. 25, no. 9, pp.522–530, 2013.

[16]. Z. E. Rosenblatt E, "Radiotherapy in cancer care: Facing the global challenge," International Atomic Energy Agency, Tech. Rep., 2017.

[17]. C. Veiga, J. McClelland, Et. Al., "Toward adaptive radiotherapy for head and neck patients: Feasibility study on using ct-to-cbct deformable registration for 'dose of the day' calculations," Med. Phys, vol. 41, no. 3, p. 031703 (12pp.), 2014.
[18]. Yngve Mardal Moe, Et. Al., "Deep learning for automatic tumour segmentation in PET/CT images of patients with head and neck cancers "
[19]. Stanislav Nikolov, Et. Al., "Deep learning to achieve clinically applicable segmentation of head and neck anatomy for radiotherapy."
[20]. Automatic Head and Neck Tumor Segmentation in PET/CT with Scale Attention Network Yading Yuan Department of Radiation Oncology Icahn School of Medicine at Mount Sinai New York, NY, USA.
[21]. Ian J. Goodfellow, Et. Al., "Generative Adversarial Networks"
[22]. Marco Domenico Cirillo, David Abramian, Anders Eklund "Vox2Vox: 3D-GAN for Brain Tumour Segmentation."
[23]. Jun Ma, et al. "Combining CNN and Hybrid Active Contours for Head and Neck Tumor Segmentation in CT and PET images", 2020, Nanjing University
[24]. Jason Brownlee, "A Gentle Introduction to Pix2Pix Generative Adversarial Network", 2019, machinelearningmastery in Generative Adversarial Network.
[25]. B. H. Menze, A. Jakab, S. Bauer, J. Kalpathy-Cramer, K. Farahani, et al., "The Mulimodal Brain Tumor Image Segmentation Benchmark (BRATS)", IEEE Transactions on Medical Imaging 34(10), 1993-2024 (2015) DOI: 10.1109/TMI.2014.2377694
[26]. S. Bakas, H. Akbari, A. Sotiras, M. Bilello, M. Rozycki, J.S. Kirby, et al., "Advancing the Cancer Genome Atlas glioma MRI collections with expert segmentation labels and radiomic features", Nature Scientific Data, 4:170117 (2017) DOI: 10.1038/sdata.2017.117
[27]. S. Bakas, M. Reyes, A. Jakab, S. Bauer, M. Rempfler, A. Crimi, et al., "Identifying the Best Machine Learning Algorithms for Brain Tumor Segmentation, Progression Assessment, and Overall Survival prediction in the BRATS Challenge", arXiv preprint arXiv:1811.02629